JOURNAL OF Materials CHEMISTRY

Crystal structure and magnetic properties of $[Fe\{N(CN)_2\}_2(MeOH)_2]$ a 2-D layered network consisting of hydrogen-bonded 1-D chains

Jamie L. Manson, Atta M. Arif and Joel S. Miller*

Department of Chemistry, University of Utah, 315 S. 1400 E. RM Dock, Salt Lake City, UT 84112–0850 USA

Received 19th October 1998, Accepted 1st February 1999

A novel 2-D layered network structure $[Fe\{N(CN)_2\}_2(MeOH)_2]$ was synthesized and characterized by X-ray crystallography, vibrational, and magnetic susceptibility. The neutral 2-D stair-like framework consists of hydrogen-bonded infinite 1-D $\{Fe[N(CN)_2]_2\}$ ribbons that pack in a staggered arrangement where nearest-neighboring chains are slipped $a/2$ relative to one another. Two methanol molecules are coordinated to the Fe^{II} center *via* the oxygen atoms in a *trans* configuration resulting in a compressed FeN_4O_2 octahedron. Hydrogen-bond interactions occur *via* N(2)···H(1)–O(1) where N(2) is the amide nitrogen atom of a nearby ribbon. The magnetic susceptibility was interpreted according to an $S=2$ expression which includes the Weiss constant and zero-field splitting giving $g=2.04$, $\theta=-2.0$ K, and $D=-1.7$ K. Intrachain exchange interactions were determined from a fit to an $S=2$ antiferromagnetic chain model leading to $g=2.04$ and $J/k_B=-0.23$ K. Further interchain interaction *via* the hydrogen bond was determined by incorporation of a molecular-field correction term yielding $J'/k_B=-0.02$ K indicating very weak antiferromagnetic coupling between chains.

Introduction

The physical properties of reduced dimensional solids comprised of covalently bonded transition metals and polyatomic organic ligands are of great interest to chemists, physicists, and theorists. One-dimensional metal complexes provide a basis for studying more complex 3-D network solids. Several examples exhibit cooperative magnetic behavior and 3-D long-range ordering, albeit at low temperatures.[1] Interestingly, 1-D chain compounds such as $[Fe(C_5Me_5)_2]^{+\cdot}[TCNE]^{-\cdot}$ [2a,b] (TCNE = tetracyanoethylene) and $Mn^{II}Cu^{II}(pbaOH)(H_2O)_3$ [2c] [pbaOH = 1,3-propylenebis(oxamate)] are among the first examples of molecule-based magnets, and exhibit ferro- and ferri-magnetic ordering at 4.8 and 4.6 K, respectively. Cyanocarbon radical anions and nitronyl nitroxides have been utilized as bridging units between metal centers so as to assemble coordination solids of 1 and 2 dimensions. For example, a class of materials based upon $[Mn^{III}(porphyrinate)]^+[TCNE]^-$ consist of alternating 1-D $S=2$ donor and $S=1/2$ acceptor chains and ferrimagnetically order at critical temperatures as high as 16 K.[3] Recently, the structure and magnetic properties of a 1-D zigzag metal complex, $[Mn(NITIm)(NITmH)]ClO_4$ [NITIm = 2-(2-imidazolyl)-4,4,5,5-tetramethyl-4,5-dihydro-1*H*-imidazole 3-oxide 1-oxyl], which is comprised of high-spin $S=5/2$ Mn^{II} and chelating imidazole-substituted nitronyl nitroxide $S=1/2$ radicals, was reported.[4] Bulk magnetic ordering was observed at 4.5 K as a result of strong antiferromagnetic intra- and inter-chain interactions (J/k_B) of -49 and -86 K, respectively.

Dicyanamide, $[N(CN)_2]^-$, possesses several possible coordination modes, and thus provides a suitable 'building block' for assembling novel inorganic/organic hybrid materials. Monodentate (terminal) coordination (**1a**) occurs in $[Cu^{II}(o\text{-phen})_2\{N(CN)_2\}][C(CN)_3]$[5a] and $[Cu^{II}(o\text{-phen})_2\{N(CN)_2\}_2]$[5b] (*o*-phen = *o*-phenanthroline). Bidentate coordination (**1b**) has been observed most often and was reported for $Me_2Sn[N(CN)_2]_2$,[5c] $Me_3Sn[N(CN)_2]$,[5c] two polymorphs of $Ag[N(CN)_2]$,[5d,e] and $Mn[N(CN)_2]_2(pyz)$ (pyz = pyrazine).[5f] The other possible bidentate coordinative mode (**1c**) has yet to be confirmed, although it is postulated for one isomer of $Cu^{II}[N(CN)_2]_2(iz)_2$ (iz = imidazole).[5g] Three-coordinate μ_3-$[N(CN)_2]^-$ (**1d**) is observed in the rutile-type class of molecule-based magnets, $M^{II}[N(CN)_2]_2$ (M = Co or Ni), that have recently been reported by us.[5h] Unusual μ_4 coordination (**1e**) is also known and was found in the structures of $Me_2Tl[N(CN)_2]$[5i] and $Na[N(CN)_2]$.[5j] In these materials, σ-bond formation occurs through lone pair donation of the terminal nitrile N atoms to an octahedral metal center. Linear 1-D chain structures of the type $M^{II}[N(CN)_2]_2L_2$ (M = Co, Ni, or Cu; L = substituted imidazoles or pyridines) have been postulated, however the extent of characterization has been primarily limited to optical and EPR studies.[6–9] With this limited knowledge in mind, our goal was to prepare and characterize new low-dimensional solids consisting of divalent transition metal complexes and the dicyanamide ligand. Herein, we report the synthesis, crystal structure, vibrational and magnetic properties of $[Fe^{II}\{N(CN)_2\}_2(MeOH)_2]$, the first structurally characterized iron(II) dicyanamide complex.

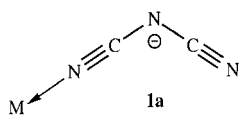

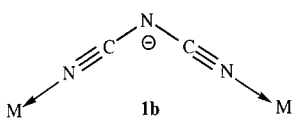

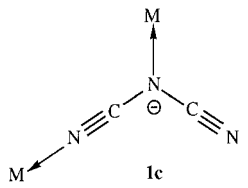

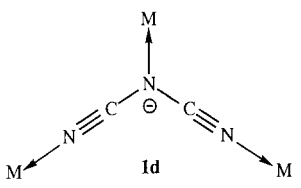

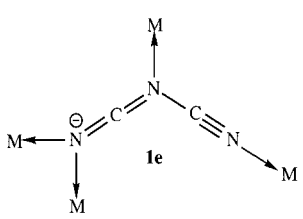

Experimental

Double-deionized water and methanol were used without further purification. The compounds $[Fe^{II}(OH_2)_6][BF_4]_2$ and $Na[N(CN)_2]$ were purchased from Aldrich and used as received.

Synthesis of *trans*-$[Fe^{II}\{N(CN)_2\}_2(MeOH)_2]$

Slow addition of a 3 mL methanolic solution of $[Fe(OH_2)_6][BF_4]_2$ (0.885 mmol, 0.2986 g) to a 5 mL aqueous solution of $Na[N(CN)_2]$ (2.28 mmol, 0.2027 g) afforded a colorless solution. Large colorless block crystals were obtained by slow solvent evaporation over a 4 d period and were collected *via* careful vacuum filtration (0.1940 g, 87%). If completely dried the crystals lose solvent and become orange suggesting oxidation of Fe^{II} to Fe^{III}. $\tilde{\nu}_{CN}$ (Nujol): 2390w, 2306m(sh), 2274m(sh), 2254s, 2178s, and 2154m cm^{-1}.

Infrared spectroscopy

Infrared spectra were recorded on a Bio-Rad Model FTS-40 spectrophotometer with $\pm 2\ cm^{-1}$ resolution in the range 4000 to 400 cm^{-1}. Samples were prepared as Nujol or Fluorolube mulls between NaCl plates.

Magnetic measurements

Dc Magnetization measurements were carried out between 2 and 300 K utilizing a Quantum Design MPMS-5XL SQUID ac/dc magnetometer equipped with a reciprocating sample operation (RSO) transport, enhanced low temperature thermometry, and magnet reset. Owing to the ease of solvent loss, some supernatant was required during sample preparation. Actual solid samples weighing approximately 15 to 25 mg, were loaded in airtight Delrin® holders and mounted on a carbon fiber rod. Measurements between 2 and 300 K were performed upon initial cooling in zero field from 300 down to 2 K and data collected on warming in a 1000 Oe dc field. Magnetic data were corrected for core diamagnetism (-176×10^{-6} emu mol^{-1}) as calculated from Pascal's constants.

Crystal structure determination

Crystallographic data, bond lengths, and bond angles are given in Tables 2 and 3. A colorless $0.30\times0.30\times0.25$ mm block of $[Fe\{N(CN)_2\}_2(MeOH)_2]$ was selected for structure determination. Owing to solvent dependence, the crystal was removed quickly from the supernatant and sealed in an epoxy matrix prior to mounting on a glass fiber. Data collection was carried out on an Enraf-Nonius CAD4 automated X-ray diffractometer at $-80\ ^{\circ}C$. Graphite-monochromated Mo-Kα radiation ($\lambda=0.71703$ Å) was used and the unit cell parameters were determined by least-squares refinement of 25 reflections. A total of 826 reflections were collected in the $4\leqslant2\theta\leqslant60^{\circ}$ range, of those 792 were unique ($R_{int}=0.0418$) and 782 observed [$I>2\sigma(I)$]. The systematic absences are unique to the *Cm* and *C*2 space groups. Attempts to solve the structure in *Cm* failed and yielded unsatisfactory results. No decay correction was applied based upon minimum reduction of standard intensities. Semiempirical absorption corrections were applied to all data using the Ψ-scan technique. The structure was solved using direct methods, completed by subsequent Fourier difference maps and refined by full-matrix least-squares procedures with the SHELXL97 Software Package.[10] All non-hydrogen atoms were refined anisotropically while methyl hydrogens were placed at calculated positions with fixed thermal parameters; H(1) was located by Fourier difference maps and refined isotropically.

Full crystallographic details, excluding structure factors, have been deposited at the Cambridge Crystallographic Data Centre (CCDC). See Information for Authors, 1999, Issue 1. Any request to the CCDC for this material should quote the full literature citation and the reference number 1145/144.

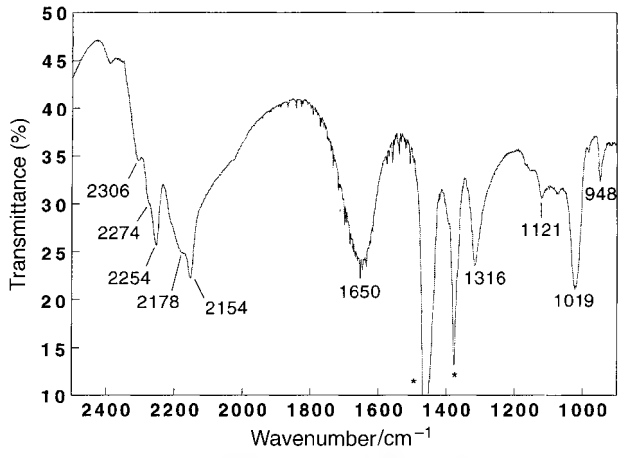

Fig. 1 The IR spectrum of $[Fe\{N(CN)_2\}_2(MeOH)_2]$ obtained as a Nujol (*) mull.

Results and discussion

Vibrational analysis

At room temperature, the solid state infrared spectrum depicts several ν_{CN} bands at 2390w, 2306m(sh), 2274m(sh), 2254s, 2178s, and 2154m cm^{-1} which are attributed to $\nu_{sym}+\nu_{asym}(C{\equiv}N)$, $\nu_{asym}(C{\equiv}N)$, and $\nu_{ssym}(C{\equiv}N)$ modes, Fig. 1, and are comparable to those of related compounds, Table 1. These bands differ significantly from those of $Na[N(CN)_2]$, which are at 2179, 2232, and 2286 cm^{-1}.[15] The large number of bands found for $[Fe\{N(CN)_2\}_2(MeOH)_2]$ suggests a low symmetry coordination environment around the Fe^{II} metal center. Absorptions due to hydroxy-containing solvents, water and MeOH, appear as similar broad bands above 3100 cm^{-1} (ν_{OH}) and approximately 1600 cm^{-1} (δ_{OH}). However, the in-plane C–H bending mode is observed at 1019 cm^{-1} and is consistent with the presence of MeOH.

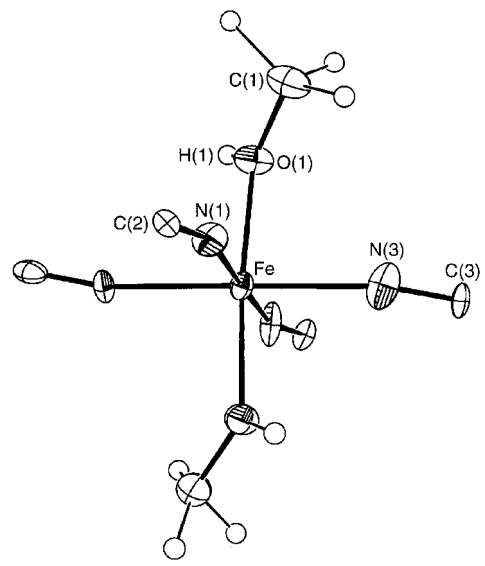

Fig. 2 The ORTEP and atom labeling diagram for $[Fe\{N(CN)_2\}_2(MeOH)_2]$. Thermal ellipsoids are shown at the 35% probability level.

Table 1 Comparison of ν_{CN} absorptions of selected $M^{II}[N(CN)_2]_2L_2$ materials

Complex	$\nu_{asym}^- + \nu_{sym}^-$ (C≡N)	ν_{asym} (C≡N)	ν_{sym} (C≡N)	Ref.
$Mn[N(CN)_2]_2(py)_2$	2295s	2234m	2167s	14
$Fe[N(CN)_2]_2(MeOH)_2$	2306m(sh), 2274m(sh)	2254s	2178s, 2154m	This work
$Co[N(CN)_2]_2(pz)_2$	2281vs	2245vs	2180vs	7
$Co[N(CN)_2]_2(iz)_2$	2281s	2246s	2185vs	9
$Co[N(CN)_2]_2(4\text{-meiz})_2$	2275s	2236s	2171vs	9
$Co[N(CN)_2]_2(2\text{-meiz})_2$	2279s	2235(sh)	2212vs, 2165vs	9
$Ni[N(CN)_2]_2(pz)_2$	2282s	2248s	2179vs, 2139vs	7
$Ni[N(CN)_2]_2(biz)_2$	2284s	2243vs	2180vs	12
$Ni[N(CN)_2]_2(tetramepz)_2$	2285vs	2250s	2180vs, 2150w	7
$Cu[N(CN)_2]_2(pz)_2$	2296s	2240s	2182vs	8
$Cu[N(CN)_2]_2(iz)_2$	2292s	2240vs	2180vs	6
$Cu[N(CN)_2]_2(3\text{-mepz})_2$	2273s	2240m	2173s	7
$Cu[N(CN)_2]_2(2\text{-mepy})_2$	2265m	2245m	2185s	13
$Pd[N(CN)_2]_2\{P(C_6H_5)_3\}_2$	2310m	2250m	2190s	11

py = Pyridine, MeOH = methanol, pz = pyrazole, iz = imidazole, 4-meiz = 4-methylimidazole, 2-meiz = 2-methylimidazole, biz = benzimidazole, tetramepz = tetramethylpyrazole, 3-mepz = 3-methylpyrazole, 2-mepy = 2-methylpyridine.

Crystal structure

The complex $[Fe\{N(CN)_2\}_2(MeOH)_2]$ crystallizes in the *C*2 space group with two molecules per unit cell. The Fe^{II} center resides on the 2-fold axis along *b* and is the only atom that occupies a special position. Fig. 2 shows an ORTEP[16] diagram of the the first coordination sphere of the Fe^{II} site and atom labeling. Compressed FeN_4O_2 octahedra consist of four different bidentate Fe–N≡C–N–C≡N–Fe bridging units and two *trans*-coordinated methanol molecules. Each octahedron is pseudo-edge-sharing with each nearest-neighbor affording rigid 1-D ribbons parallel to the crystallographic *c*-axis. The Fe–N(1) and Fe–N(3) bond distances are 2.161(7) and 2.137(7) Å, respectively, while Fe–O(1) is substantially shorter at 2.099(2) Å. Approximate C_{2v} symmetry is observed for the $[N(CN)_2]^-$ ligand with C(2)–N(1) and C(3)–N(3) bond distances of 1.14(1) and 1.18(1) Å, respectively. The lack of significant electron density near the amide nitrogen N(2) results in longer N(2)–C(2) and N(2)–C(3) bond distances which average 1.31 Å, suggesting a small degree of π conjugation within the $[N(CN)_2]^-$ backbone. Distortions from 90° are noted in the FeN_4 equatorial plane with N(3)–Fe–N(1) and N(3)–Fe–N(3^I) bond angles of 92.3(1) and 87.4(2)°. The observed metal–nitrile bond angles deviate appreciably from linearity but are typical of this bonding configuration.[5h,14,17,18] Owing to staggered packing of the linear 1-D chains, extended 2-D stair-like layers are produced which are held together *via* N(2)···H(1)–O(1) hydrogen bonds with a bond distance of 1.883 Å and forming an angle of 177.4°, Figs. 3 and 4. Intra- and interchain Fe···Fe separations are 7.392 and 7.283 Å, respectively.

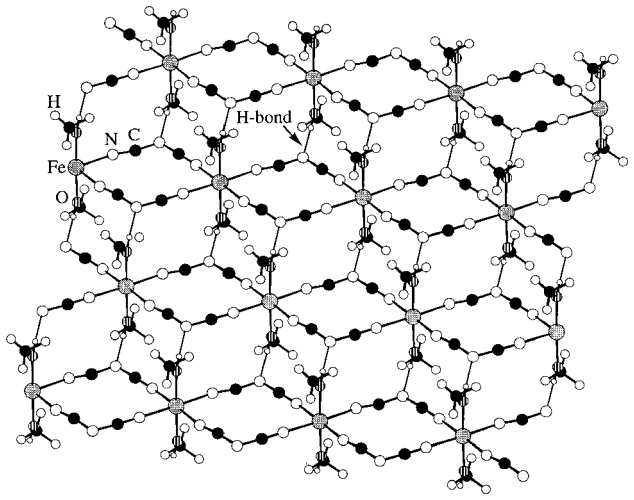

Fig. 3 Extended 2-D layered structure of $[Fe\{N(CN)_2\}_2(MeOH)_2]$ showing the hydrogen bonding between linear chains.

Table 2 Summary of the crystallographic data for $[Fe\{N(CN)_2\}_2(MeOH)_2]$

Empirical formula	$C_6H_8FeN_6O_2$
M	252.02
Crystal symmetry	Monoclinic
Space group	*C*2 (no. 5)
a/Å	12.271(3)
b/Å	7.392(2)
c/Å	6.478(2)
β/°	120.40(2)
V/Å^3	506.86(3)
Z	2
D_c/g cm^{-3}	1.651
μ/cm^{-1}	14.758
R	0.0416
*wR*2	0.0608

Table 3 Selected bond distances (Å) and bond angles (°) for $[Fe\{N(CN)_2\}_2(MeOH)_2]$

Fe–O(1)	2.099(2)	N(1)–C(2)	1.14(1)
Fe–N(1)	2.161(7)	N(2)–C(2)	1.33(1)
Fe–N(3)	2.137(7)	N(2)–C(3)	1.29(1)
O(1)–C(1)	1.419(4)	N(3)–C(3)	1.18(1)
Fe···Fe[a]	7.392	Fe···Fe[b]	7.283
N(2)···H(1)–O(1)[c]	1.883		
O(1)–Fe–N(1)	92.2(3)	C(2)–N(2)–C(3)	117.8(3)
O(1)–Fe–N(3)	87.9(3)	Fe–N(3)–C(3)	163.0(7)
N(1)–Fe–N(3)	92.3(1)	N(1)–C(2)–N(2)	173.5(7)
Fe–O(1)–C(1)	131.3(2)	N(2)–C(3)–N(3)	171.2(8)
Fe–N(1)–C(2)	158.0(7)	N(2)···H(1)–O(1)[c]	177.4

[a]Intrachain separation. [b]Interchain separation. [c]Hydrogen-bonding interaction.

Magnetic properties

The magnetic susceptibility, χ, of $[Fe\{N(CN)_2\}_2(MeOH)_2]$ has been measured between 2 and 300 K. The room temperature effective moment is 5.03 μ_B and slightly higher than the predicted value (4.90 μ_B) for isolated $S=2$ metal ions. The moment remains constant until approximately 50 K and decreases rapidly down to 2 K (3.18 μ_B) due to antiferromagnetic coupling and effects of zero-field splitting. High-spin, octahedral Fe^{II} ($S=2$) possesses a $^5T_{2g}$ ground state, and as a result effects due to zero-field splitting are anticipated at low temperature.[19] The data were fitted by the Curie–Weiss expression, $\chi \propto (T-\theta)^{-1}$, with $g=2.04$ and $\theta=-2.70$ K, however in this case θ also includes the contribution from zero-field splitting, *D*, and is thus overestimated. Therefore *D* was

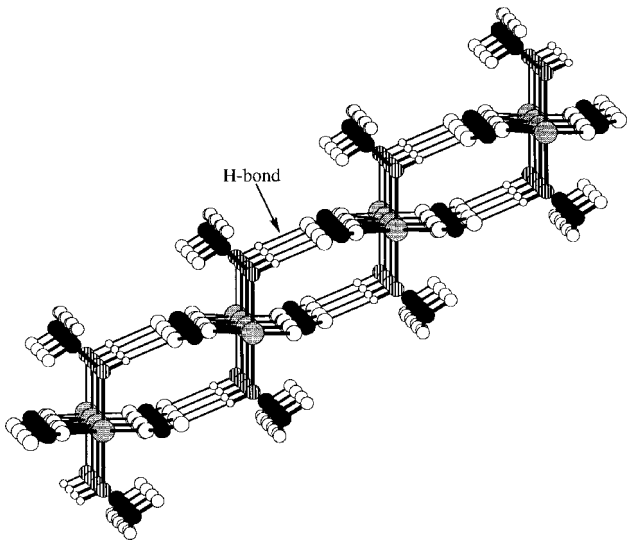

Fig. 4 Alternative view of the structure of $[Fe\{N(CN)_2\}_2(MeOH)_2]$ depicting the stair-like layer packing motif.

determined by fitting eqn. (1) (using the Hamiltonian, $H = DS_z^2 + g\beta H \cdot S$) to the magnetic data yielding $g = 2.04$, $\theta = -2.0$ K, and $D = -1.7$ K, Fig. 5.[20]

$$\mu^2 = \frac{6g^2\,(e^{-D/T} + 4e^{-4D/T})}{1 + 2e^{-D/T} + 2e^{-4D/T}} + \frac{2g^2 k_B T(18 - 14e^{-D/T} - 4e^{-4D/T})}{D(1 + 2e^{-D/T} + 2e^{-4D/T})} \quad (1)$$

Lande g values in excess of 2.0 are expected for the Fe^{II} ion as a result of the $^5T_{2g}$ electronic state, and the value of D is well within the range expected for six-coordinate high-spin Fe^{II} complexes. Values as large as -29.7 K have been reported for complexes such as $Fe^{II}_{1-x}Zn_xSiF_6 \cdot 6H_2O$.[21]

In order to determine the intrachain exchange parameter, J/k_B, through the –NCNCN– bridges, the susceptibility was also fitted by the $S = 2$ 1-D chain expression of Hiller *et al.*,[22] eqn. (2) (Fig. 5), giving $g = 2.04$ and $J/k_B = -0.23$ K indicative of weak antiferromagnetic interactions between well separated Fe^{II} metal centers.

$$\chi_{1-D} = \frac{Ng^2\mu_B^2(2 + 71.938x^2)}{(1 + 10.482x + 955.56x^3)k_B T} \quad (2)$$

where $x = |J|/k_B T$, N = Avogadro's number, g = Landé g value, μ_B = Bohr magneton, and k_B = Boltzmann's constant. To elucidate the significance of the exchange *via* the N(2)···H(1)–O(1) hydrogen bond, *i.e.* the 2-D interchain interaction, a molecular field correction term was also included, eqn. (3), which gave $g = 2.04$ and $J'/k_B = -0.02$ K, suggestive of very weak (and perhaps negligible) antiferromagnetic interchain interactions.[22]

$$\chi_{MF} = \frac{\chi_{1-D}}{[1 - \chi_{1-D}(2zJ'/Ng^2\mu_B^2)]} \quad (3)$$

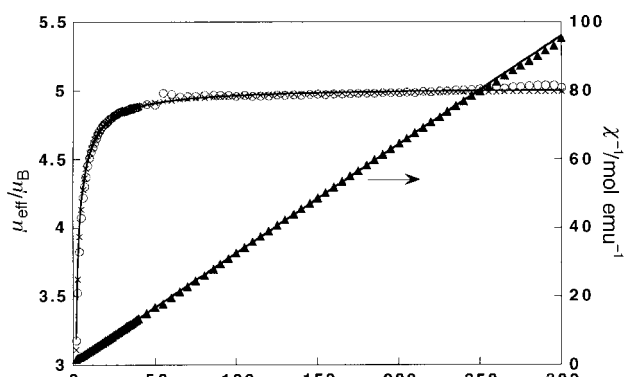

Fig. 5 Temperature dependence of the effective moment (○) and reciprocal molar magnetic susceptibility (▲). The data were fitted by the $S = 2$ 1-D antiferromagnetic chain model (—) giving $g = 2.04$ and $J/k_B = -0.23$ K [eqn. (2)]. Incorporation of a zero-field splitting term (x) yielded $g = 2.04$, $\theta = -2.0$ K, and $D = -1.7$ K [eqn. (1)].

Conclusion

A novel 2-D layered structure consisting of hydrogen-bonded 1-D $\{Fe[N(CN)_2]_2\}$ linear chains has been described. The use of hydrogen-bonding interactions is an efficient way of increasing the structural dimensionality of inorganic/organic hybrid materials which is key to enhancing spin coupling. Surprisingly, the exchange interaction *via* hydrogen bonds was determined to be very weak and contributes little to the overall magnetic properties.

Acknowledgements

The authors gratefully acknowledge the American Chemical Society–Petroleum Research Fund (Grant No. 30722-AC5) and the U. S. Department of Energy (Grant No. DE-FG03–93ER45504) for support of this work.

Note added at proof: $Mn[N(CN)_2]_2(MeOH)_2 \cdot 2Me_2CO$ was recently reported to order as a canted antiferromagnet below T_c of 16.0 K.[24] Since the related $Fe[N(CN)_2]_2(MeOH)_2$ does not magnetically order, we believe that the magnetic ordering is solely due to the desolvation product $Mn[N(CN)_2]$ which magnetically orders at 16 K.[25]

References

1 R. L. Carlin and F. Palacio, *Coord. Chem. Rev.*, 1985, **65**, 141; R. L. Carlin, *J. Chem. Educ.*, 1991, **68**, 361.
2 (*a*) J. S. Miller, J. C. Calabrese, A. J. Epstein, R. W. Bigelow, J. H. Zhang and W. M. Reiff, *J. Chem. Soc., Chem. Commun.*, 1986, 1026; (*b*) J. S. Miller, J. C. Calabrese, H. Rommelmann, S. R. Chittipeddi, J. H. Zhang, W. M. Reiff and A. J. Epstein, *J. Am. Chem. Soc.*, 1987, **109**, 769; (*c*) Y. Pei, M. Verdaguer and O. Kahn, *J. Am. Chem. Soc.*, 1986, **108**, 428.
3 (*a*) J. S. Miller, J. C. Calabrese, R. S. McLean and A. J. Epstein, *Adv. Mater.*, 1992, **4**, 498; (*b*) J. S. Miller and A. J. Epstein, *Chem. Commun.*, 1998, 1319.
4 K. Fegy, D. Luneau, E. Belorizky, M. Novac, J.-L. Tholence, C. Paulsen, T. Ohm and P. Rey, *Inorg. Chem.*, 1998, **37**, 4524.
5 (*a*) I. Potocnák, M. Dunaj-Jurco, D. Miklos and L. Jäger, *Acta Crystallogr., Sect. C*, 1996, **52**, 1653; (*b*) I. Potocnák, M. Dunaj-Jurco, D. Miklos and M. Kabesová, *Acta Crystallogr., Sect. C*, 1995, **51**, 600; (*c*) Y. M. Chow, *Inorg. Chem.*, 1971, **10**, 1938; (*d*) Y. M. Chow and D. Britton, *Acta Crystallogr., Sect. B*, 1977, **33**, 697; (*e*) D. Britton, *Acta Crystallogr., Sect. C*, 1990, **46**, 2297; (*f*) J. L. Manson, C. D. Incarvito, A. L. Rheingold and J. S. Miller, *J. Chem. Soc., Dalton Trans.*, 1998, 3705; (*g*) J. Mrozinski, M. Hvastijová and J. Kohout, *Polyhedron*, 1992, **11**, 2867; (*h*) J. L. Manson, C. R. Kmety, Q. Huang, J. W. Lynn, G. Bendele, S. Pagola, P. W. Stephens, A. J. Epstein and J. S. Miller, *Chem. Mater.*, 1998, **10**, 2552; (*i*) Y. M. Chow and D. Britton, *Acta Crystallogr., Sect. B*, 1975, **31**, 1934; (*j*) J. L. Manson, C. F. Campana and J. S. Miller, unpublished results.
6 H. Köhler, H. Hartung and B. Seifert, *Z. Anorg. Allg. Chem.*, 1966, **347**, 30.
7 M. Hvastijová, J. Kohout, H. Köhler and G. Ondrejovic, *Z. Anorg. Allg. Chem.*, 1988, **566**, 111.
8 J. Mrozinski, J. Kohout, M. Hvastijová and H. Köhler, *Transition Met. Chem.*, 1986, **11**, 481.
9 M. Hvastijová, J. Kozisek, J. Kohout, L. Jäger and H. Fuess, *Transition Met. Chem.*, 1995, **20**, 276.
10 SHELX97 Programs for Crystal Structure Analysis (Release 97-2), University of Göttingen, Germany, 1997.
11 H. Köhler, H. Wusterhausen, M. Jeschke and A. Kolbe, *Z. Anorg. Allg. Chem.*, 1987, **547**, 69.
12 M. Hvastijová, J. Kohout, M. Okruhlica, J. Mrozinski and L. Jäger, *Transition Met. Chem.*, 1993, **18**, 579.

13 M. Hvastijová, J. Kohout, H. Wusterhausen and H. Köhler, *Z. Anorg. Allg. Chem.*, 1984, **510**, 37.
14 J. L. Manson, A. M. Arif, C. D. Incarvito, L. M. Liable-Sands, A. L. Rheingold and J. S. Miller, submitted.
15 H. Köhler, A. Kolbe and G. Lux, *Z. Anorg. Allg. Chem.*, 1977, **428**, 103.
16 ORTEP3 for Windows, L. J. Farrugia, *J. Appl. Crystallogr.*, 1997, **30**, 565.
17 J. L. Manson, D. W. Lee, A. L. Rheingold and J. S. Miller, *Inorg. Chem.*, 1998, **37**, 5966.
18 J. Kozisek, H. Paulus, M. Dankova and M. Hvastijová, *Acta Crystallogr., Sect. C*, 1996, **52**, 3019.
19 R. L. Carlin, *Magnetochemistry*, Springer, Berlin, 1986, ch. 2.
20 D. V. Behere and S. Mitra, *Inorg. Chem.*, 1980, **19**, 992.
21 F. Varret, Y. Allain and A. Miedan-Gros, *Solid State Commun.*, 1974, **14**, 17; F. Varret, *J. Phys. Chem. Solids*, 1976, **37**, 257.
22 W. Hiller, J. Strahle, A. Datz, M. Hanack, W. F. Hatfield and P. Gutlich, *J. Am. Chem. Soc.*, 1984, **106**, 329.
23 B. E. Myers, L. Berger and S. A. Friedberg, *J. Appl. Phys.*, 1968, **40**, 1149.
24 M. Kurmoo and C. J. Kepert, *New J. Chem.*, 1998, **22**, 1515.
25 L. Manson, C. R. Kmety, A. J. Epstein and J. S. Miller, submitted.

Paper 8/08089E